Advances in Experimental Medicine and Biology 1077

Heung Jae Chun · Kwideok Park
Chun-Ho Kim · Gilson Khang *Editors*

Novel Biomaterials for Regenerative Medicine

Springer

Advances in Experimental Medicine and Biology

Volume 1077

More information about this series at http://www.springer.com/series/5584

Heung Jae Chun • Kwideok Park
Chun-Ho Kim • Gilson Khang
Editors

Novel Biomaterials for Regenerative Medicine

Springer

Editors
Heung Jae Chun
The Catholic University of Korea
Seoul, South Korea

Chun-Ho Kim
Korea Institute of Radiological
and Medical Sciences
Seoul, South Korea

Kwideok Park
Korea Institute of Science
and Technology
Seoul, South Korea

Gilson Khang
Chonbuk National University
Jeonju, South Korea

ISSN 0065-2598 ISSN 2214-8019 (electronic)
Advances in Experimental Medicine and Biology
ISBN 978-981-13-0946-5 ISBN 978-981-13-0947-2 (eBook)
https://doi.org/10.1007/978-981-13-0947-2

Library of Congress Control Number: 2018952634

This Springer imprint is published by the registered company Springer Nature Singapore Pte Ltd.
The registered company address is: 152 Beach Road, #21-01/04 Gateway East, Singapore 189721, Singapore

Preface

Regenerative medicine is a branch of multidisciplinary research in tissue engineering and molecular biology, which deals with the process of replacing, engineering, or regeneration of human cells, tissues, or organs to restore or establish normal function. Regenerative medicine is leading the innovation of life sciences and medicine with various expansion toward stem cells, cell therapy, and tissue engineering, and hence it is now becoming a pillar of the advanced medical industry. In regeneration medicine fields, biomaterials are essential tools for replacing part of a living system or to function in intimate contact with the living tissue. Therefore, this book introduces the recent trends of biomaterials derived either from nature or synthesized in the laboratory using a variety of chemical approaches utilizing metallic components, polymers, ceramics, or composite materials. The book consists of 5 main parts and 28 chapters containing recent topics reported by a number of prominent researches in these fields.

Part I reviews the fate of stem cells regulated by biomaterials.

Chapter 1 is an introduction to the human placenta laminin-111 as a multifunctional protein for tissue engineering and regenerative medicine. In Chap. 2, a novel strategy for simple and robust expansion of human pluripotent stem cells using botulinum hemagglutinin is introduced. Polycaprolactone scaffolds used for the growth and differentiation of dental stem cells of apical papilla are summarized in Chap. 3. The impact of three-dimensional culture systems on hepatic differentiation of pluripotent stem cells and beyond is introduced in Chap. 4.

Controlling of signal pathway of stem cell by biomaterials is discussed in Part II.

In Chap. 5, modulation of the osteoimmune environment in the development of biomaterials for osteogenesis is reviewed. For tissue regeneration and disease modeling, novel biomimetic microphysiological systems are summarized in Chap. 6. Chapter 7 contains the feasibility of silk fibroin in wound healing process. In Chap. 8, the role of natural-based biomaterials in advanced therapies for autoimmune diseases is described.

Part III describes functional biomaterials for regenerative medicine.

Content of Chap. 9 includes recent advancements in decellularized matrix-based biomaterials for musculoskeletal tissue regeneration. In Chap. 10, clinical applications of injectable biomaterials are introduced. Advanced injectable alternatives for osteoarthritis are discussed in Chap. 11. Chapters 12, 13 and 14 introduce fabrication of hydrogel materials, injectable nanocomposite hydrogels and electrosprayed nano(micro)particles, and advances in waterborne polyurethane-based biomaterials for biomedical applications, respectively. Content reviewed in Chap. 15 is medical applications of collagen and hyaluronan in regenerative medicine.

Part IV shows the review on inorganic biomaterials for regenerative medicine.

Calcium phosphate biomaterials for clinical application in dentistry are described in Chap. 16. In Chap. 17, stem cell and advanced nano bioceramic interactions are discussed. Chap. 18 introduces recent trend in hydroxyapatite (HAp) synthesis and the synthesis report of nanostructure HAp by hydrothermal reaction. Use of TiO_2 in the bone regeneration is discussed in Chap. 19.

Finally, **Part V introduces the recent trends of smart natural biomaterials for regenerative medicine**.

Chapter 20 reviews the feasibility of silk fibroin-based scaffold for bone tissue engineering. Chapter 21 explains characteristics of collagen Type I as a versatile biomaterial. Techniques of tissue-inspired interfacial coatings for regenerative medicine are described in Chap. 22. Chapters 23, 24 and 25 introduce naturally derived biomaterials, mussel-inspired biomaterials, and chitosan for tissue engineering applications, respectively. Chapter 26 reviews demineralized dentin matrix (DDM) as a carrier for recombinant human bone morphogenetic proteins (rhBMP-2). Prospects of natural polymeric scaffolds in peripheral nerve tissue regeneration are introduced in Chap. 27. In Chap. 28, chitosan-based dressing materials for problematic wound management are reviewed.

We offer a special thanks to all participants who have generously devoted their time, energy, experience, and intelligence for successful completion of this book. Their efforts will contribute to next generation who studies regenerative medicine based on biomaterials. Finally, we really appreciate the effort of Dr. Sue Lee, the publishing editor of biomedical sciences of Springer Nature, who made a great effort to publish this book. Also we would like to appreciate Mrs. Ok Kyun Choi and Yong Woon Jeong at Gilson's Lab for e-mailing all authors, editing, pressing, and so on as boring

and tedious works. Without their support, this huge work would not have been possible.

Acknowledgement This research was supported by the Basic Science Research Program through the National Research Foundation of Korea (NRF), funded by the Ministry of Science, ICT and Future Planning (NRF-2017R1A2B3010270), and the Korea Health Technology R&D Project through the Korea Health Industry Development Institute (KHIDI), funded by the Ministry of Health and Welfare.

Seoul, South Korea — Heung Jae Chun, Kwideok Park, Chun-Ho Kim

Jeonju, South Korea — Gilson Khang

Contents

Part III Functional Biomaterials for Regenerative Medicine

Part IV Inorganic Biomaterials for Regenerative Medicine

Part I

The Fate of Stem Cell by Biomaterials

1 Human Placenta Laminin-111 as a Multifunctional Protein for Tissue Engineering and Regenerative Medicine

Johannes Hackethal, Christina M. A. P. Schuh, Alexandra Hofer, Barbara Meixner, Simone Hennerbichler, Heinz Redl, and Andreas H. Teuschl

Abstract

Laminins are major components of all basement membranes surrounding nerve or vascular tissues. In particular laminin-111, the prototype of the family, facilitates a large spectrum of fundamental cellular responses in all eukaryotic cells. Laminin-111 is a biomaterial frequently used in research, however it is primarily isolated from non-human origin or produced with time-intensive recombinant techniques at low yield.

Here, we describe an effective method for isolating laminin-111 from human placenta, a clinical waste material, for various tissue engineering applications. By extraction with Tris-NaCl buffer combined with non-protein-denaturation ammonium sulfate precipitation and rapid tangential flow filtration steps, we could effectively isolate native laminin-111 within only 4 days. The resulting material was biochemically characterized using a combination of dot blot, SDS-PAGE, Western blot and HPLC-based amino acid

The work was performed at the Ludwig Boltzmann Institute for Experimental and Clinical Traumatology; Austrian Cluster for Tissue Regeneration, Donaueschingenstraße 13, 1200 Vienna, Austria.

J. Hackethal (✉) · B. Meixner · H. Redl
Ludwig Boltzmann Institute for Experimental and Clinical Traumatology in AUVA Trauma Research Center, Vienna, Austria

Austrian Cluster for Tissue Regeneration, Vienna, Austria
e-mail: Johannes.Hackethal@trauma.lbg.ac.at

C. M. A. P. Schuh
Ludwig Boltzmann Institute for Experimental and Clinical Traumatology in AUVA Trauma Research Center, Vienna, Austria

Austrian Cluster for Tissue Regeneration, Vienna, Austria

Laboratory of Nano-Regenerative Medicine, Faculty of Medicine, Cells for Cells, Universidad de Los Andes, Santiago, Chile

A. Hofer
Research Area Biochemical Engineering, Institute of Chemical Engineering, Vienna University of Technology, Vienna, Austria

S. Hennerbichler
Austrian Cluster for Tissue Regeneration, Vienna, Austria

Red Cross Blood Transfusion Service of Upper Austria, Linz, Austria

A. H. Teuschl
Austrian Cluster for Tissue Regeneration, Vienna, Austria

Department of Biochemical Engineering, University of Applied Sciences Technikum Wien, Vienna, Austria

H. J. Chun et al. (eds.), *Novel Biomaterials for Regenerative Medicine*, Advances in Experimental Medicine and Biology 1077, https://doi.org/10.1007/978-981-13-0947-2_1

analysis. Cytocompatibility studies demonstrated that the isolated laminin-111 promotes rapid and efficient adhesion of primary Schwann cells. In addition, the bioactivity of the isolated laminin-111 was demonstrated by (a) using the material as a substrate for outgrowth of NG 108-15 neuronal cell lines and (b) promoting the formation of interconnected vascular networks by GFP-expressing human umbilical vein endothelial cells.

In summary, the isolation procedure of laminin-111 as described here from human placenta tissue, fulfills many demands for various tissue engineering and regenerative medicine approaches and therefore may represent a human alternative to various classically used xenogenic standard materials.

Keywords

Laminin-111 · Placenta · Schwann cells · NG 108-15 · Vasculogenesis

1.1 Introduction

Basement membranes (BMs) are specialized extracellular sheet-like matrices underlying epithelia in all mammals [1]. They are key elements during embryogenesis and are mainly composed of laminins, collagen-4 and heparin sulfate proteoglycans [2], joined together by nidogens, perlecans and other proteins [3].

In this regard, the primary function of laminins, a family of large heterotrimeric (a, ß, γ) glycoproteins present in BMs, is to interact with receptors anchored in the plasma membrane of cells, such as endothelial or neuronal cells [1]. Laminin-111, a 800-kDa protein, is the prototype of the family and the best characterized laminin isoform [1, 3] It is adhesive for most cell types, promotes cell survival *in vitro* and has various biological key activities [3–5], including cell adhesion, proliferation, differentiation and migration [1, 6]. Laminins are frequently used for *in vitro* and *in vivo* neuronal cell cultivation [7–11], angiogenesis [5, 12], wound healing [6, 13–15], or stem cell studies [16, 17].

Laminin-111 was the first laminin type isolated by Ruppert Timpl from Engelbreth-Holmes Sarcoma (EHS) mouse material during the 1970s [18]. For several years this has been the only known laminin isoform [19]. Since its discovery, many attempts have been made to isolate laminin-111 from a human source such as placenta [20–24] or produce it recombinantly [25, 26]. However, no human equivalent to the mouse tumor derived EHS laminin-111 is available for large-scale production and therefore, more than 30 years after its discovery, laminin-111 extracted from xenogenic EHS tumor tissue is still the frequently used gold standard for various *in vitro* and *in vivo* research protocols [27].

The aim of this study was to establish an effective method for isolation of human placental laminin-111 (pLm-111). The method was based on an extraction step via Tris-NaCl buffer to yield a laminin-rich protein fraction, followed by a protein precipitation step using 30% ammonium chloride combined with a series of diafiltration and salt precipitation steps to remove non-laminin contaminants and therefore purify the laminin-111 isolates. The resulting purified laminin-111 was biochemically characterized using a combination of dot blot, sodium dodecyl sulfate polyacrylamide gel electrophoresis (SDS-PAGE), Western blot and HPLC-based amino acid analysis. The *in vitro* biocompatibility and bioactivity of laminin-111 was demonstrated using NG 108-15 neuronal cell lines, Schwann cells and GFP-expressing human umbilical vein endothelial cells (gfpHUVEC).

1.2 Materials and Methods

If not stated otherwise all chemicals were purchased from Sigma Aldrich and of analytical grade.

1.2.1 Collection of Human Placenta Tissue

Placenta material was collected after caesarian section from the Landes-Kinderklinik Hospital Linz, Austria (with the permission of the local ethical board and informed consent from all donors), delivered to LBI Trauma laboratories on dry ice, and stored at −20 °C until the isolation procedure was performed.

1.2.2 Isolation Procedure of Placenta Laminin-111 (pLm-111)

All isolation steps were performed in a cold-room at 4 °C. For all diafiltration steps in this protocol the tangential flow filtration (TFF) Ultralab™ system PALL (VWR, Vienna, Austria) has been used, equipped with a 100 kDa cut-off Ultrasette™ tangential flow filter.

After thawing, the placenta was dissected free of the outer membranes, amnion and chorion as well as of the umbilical cord. The residual basal tissue was used for the isolation process. Blood components were removed by repetitive homogenization steps of 100 g basal placenta tissue in 200 mL phosphate buffered saline (PBS) without Ca^{2+}/Mg^{2+} using a blender (Braun Type 4184, Kronberg, Germany) and subsequent centrifugation at 3.000 × g for 5 min using a Heraeus Multifuge™ (Beckman Instruments GmbH Type 1 S-R, Vienna, Austria). The supernatant fluid containing blood components was discarded, pellets were resuspended in fresh PBS and centrifuged again (three times). Thereafter, the procedure was repeated three times with aqua dest.

Subsequently, 100 g wet weight of blood-free basal tissue were homogenized for 60 s in 100 mL Tris-NaCl buffer (50 mM Tris, 0.5 M NaCl, 4 mM EDTA, 2 mM N-Ethylmaleimide (NEM), pH 7.4) using the blender. Suspension was stirred overnight on a magnetic stirrer at 200 rpm and subsequently centrifuged at 7.000 × g for 15 min. Supernatants were collected and crystalline ammonium sulfate ($[NH_4]_2SO_4$) was added to adjust for 30% final concentration. After 2 h of stirring, the extract was centrifuged at 7.000 × g for 15 min. Pellets were collected in 150 mL Tris-buffered saline (TBS) buffer and diafiltrated against 10× volumes of TBS. To precipitate collagen-4 contaminants, NaCl concentration was adjusted to 1.7 M by adding 150 mL of 3.4 M NaCl at a constant flow rate of 2 mL/min using a Minipuls Evolution® roller pump (Gilson Inc., Vienna, Austria) and stirred overnight at 200 rpm. Subsequently, the suspension was centrifuged at 7.000 × g for another 15 min. Supernatant containing native pLm-111 was either (a) diafiltrated against at least 3 volumes of TBS and stored at −80 °C (native pLm-111), or (b) diafiltrated against aqua dest. to remove residual salts, and concentrated to approximately 200 mL using TFF, and lyophilized (Christ Alpha 1-4 lyophilizer, Heraeus Schauer GmbH, Vienna, Austria). The resulting lyophilized pLm-111 was stored at −20 °C for up to 12 months before further use.

1.2.3 Biochemical Identification of pLm-111

1.2.3.1 Dot Blots

For native pLm-111 detection, dot blots were performed. 2 µL of either 1 mg/mL EHS laminin-111, pLm-111 (native or lyophilized), collagen-1 or recombinant laminin-111 from fibroblast cell culture (Sigma Aldrich, Vienna, Austria) were pipetted in duplicates on nitrocellulose membranes (Peqlab, Erlangen, Germany) and air-dried for 60 min. Thereafter, membranes were blocked with 5% skim milk powder in TBS buffer for 60 min and incubated with 1:2000 diluted monoclonal primary laminin-111 antibodies in TBS for another 60 min. After washing with TBS, membranes were incubated with peroxidase conjugated secondary antibodies (Abcam, CA, USA) for 60 min and signals were detected using a Multiimage Light Cabinet (BioZym, NY, USA).

1.2.3.2 SDS PAGE/Western Blot

SDS PAGE and western blot analysis were performed as previously described using the XCell

SureLock™ Mini-Cell Electrophoresis System (Invitrogen, Vienna, Austria) [28, 29]. Briefly, 20 µg per lane of EHS laminin-111 (control), or lyophilized pLm-111 reconstituted in TBS buffer were resolved on 3–8% SDS-polyacrylamide gels (NuSep®, VWR, Austria), stained with 0.25% (w/v) Coomassie Brilliant Blue, or transferred onto nitrocellulose membranes (Peqlab) using the XCell II Blot Module (Invitrogen, Vienna, Austria). Membranes were blocked with 5% milk powder in TBS buffer containing 0.1% Tween (TBS/T) and incubated with anti-laminin-111 (polyconal 1:2000, AB11575, Abcam, USA) in 5% BSA-TBS/T at 4 °C overnight. Subsequently, membranes were incubated with peroxidase conjugated secondary antibodies (R1364HRP, Arctis GmbH, Germany) in 5% milk-TBS/T, and signals were detected using a Multiimage Light Cabinet (BioZym).

1.2.3.3 Amino Acid Analysis

Amino acid quantification was performed as previously described [30]. Briefly, pLm-111 was digested following a two-step protocol (enzymatical followed by chemical). 75 mg of lyophilized sample were incubated with 1 mL of 0.0125% protease from Streptomyces griseus in 1.2% TRIS/ 0.5% SDS pH 7.5 (adjusted with 0.1% HCl) solution for 72 h at 37 °C. Then 1 mL of 4% formic acid in ddH_2O was added for chemical pre-digestion and the suspension was incubated for 2 h at 108 °C followed by lyophilization. The dried samples were reconstituted in 5 mL 0.6% TRIS and 7 M guanidine hydrochloride pH 8 for 2 h. After centrifugating (Sigma centrifuge, 3–18 K) the sample at 4800 rpm for 15 min at 4 °C, 1 mL of the supernatant was combined with 0.5 mL 4 M methansulfonic acid solution containing 0.2% tryptamine and incubated for 1 h at 160 °C. Subsequently, the solution was quantitatively transferred into a 5 mL volumetric flask, 225 µL 8 M NaOH and 0.25 mL internal standard were added and the flask was filled up with 2.2 M sodium acetate solution. The samples were then directly used for HPLC analysis.

A multi-amino acid standard mix was prepared by mixing the amino acid standard, a solution containing 2.5 mM each of asparagine, glutamine and tryptophan in MQ, a solution containing 2.5 mM each of taurine and hydroxyproline in 0.1 M HCl and a solution of the internal standards, i.e. 25 mM each of norvaline and sarcosine in 0.1 M HCl. Ten different concentrations of this standard mixture, ranging between 45 mg/L and 0.5 mg/L, were used for calibration.

The HPLC system Ultimate 3000 (Thermo Fisher Scientific, USA) was equipped with a pump (LPG-3400SD), a split-loop auto-sampler (WPS-3000 SplitLoop), a column oven (Col. Comp. TCC-3000SD) and a fluorescence detector (FLD-3400RS). Chromeleon 7.2 software was used for the control of the device as well as for the quantification of the peak areas. Chromatographic separation was achieved with a reversed phase column (Agilent Eclipse AAA, 3x 150 mM, 3.5 µm) a guard column (Agilent Eclipse AAA, 4.6 × 12.5 mM, 5 µm) and a gradient using eluent (A) 40 mM NaH_2PO_4 monohydrate pH 7.8 and eluent (B) MeOH/ACN/MQ (45/45/10, v/v/v). The protocol was run at a flow-rate of 1.2 mL min^{-1}, the column oven temperature was set to 40 °C and the injection volume was 10 µL. As most amino acids have no fluorophore in their structure, an in-needle derivatization step was performed using 0.4 M borate buffer, 5 mg/mL ortho-phthalaldehyde (OPA) in 0.4 M borate buffer containing 1% of 3-MPA, 2.5 mg/mL FMOC and 1 M acetic acid for pH adjustment. In order to guarantee sample quantification despite the derivatization step, every sample was spiked with 25 mM sarcosine in 0.1 M HCl and 25 mM sorvaline in 0.1 M HCl as internal standards. Primary amines and norvaline were detected at Ex 340 nm/Em 450 nm and secondary amines and sarcosine were detected at Ex 266 nm/Em 305 nm.

1.2.4 In Vitro Biocompatibility Testing of Isolated pLm-111

All *in vitro* experiments were performed with lyophilized pLm-111.

1.2.5 Adhesion

1.2.5.1 Primary Schwann Cell Isolation

All animals were euthanized according to established protocols, which were approved by the City Government of Vienna in accordance with the Austrian Law and the Guide for the Care and Use of Laboratory Animals as defined by the National Institute of Health.

Prior to Schwann cell isolation, sciatic nerves of adult male Sprague Dawley rats were dissected and kept in PBS on ice. Schwann cell isolation was performed as previously described [31], adapted from Kaekhaw et al. [32]. Cells were cultured in DMEM-D-valine (PAA, Austria), supplemented with 10% FCS, 2 mM L-Glutamine (PAA, Austria), 1% antibiotics (PAA, Austria), N_2 supplement (Invitrogen, Germany), 10 µg/mL bovine pituitary extract and 5 µM forskolin.

1.2.5.2 Primary Schwann Cell Adhesion

For the Schwann cell culture, tissue culture plastic (TCP) was coated with poly-L-lysine and/or EHS laminin-111 or pLm-111. Briefly, 96-well plates were incubated with 0.01% (w/v) poly-L-lysine for 15 min at room temperature in a laminar flow-hood. Poly-L-lysine was removed and plates were left to dry for at least 2 h. Subsequently, wells were incubated with EHS laminin-111 or pLm-111 reconstituted in PBS (100 µg/mL) and incubated at 37 °C for 30 min. Laminin-111 solution was removed and plates were washed twice with PBS followed by UV sterilization.

Cell viability of Schwann cells on TCP, poly-L-lysin, EHS laminin-111, pLm-111 or on combinations of poly-L-Lysin with either EHS laminin-111 or pLm-111 was determined using MTT assay. Schwann cells, seeded at a density of 4×10^3cells/cm^2 (n = 18), were incubated with culture medium containing 650 µg/mL MTT [3-(4,5- dimethylthiazol-2-yl)-2,5-diphenyltetrazolium] bromide for 1 h in a cell culture incubator (37 °C, 5% CO_2 and 80% humidity). MTT reagent was discarded and MTT formazan precipitate was dissolved in 100 µL DMSO per well of a 96 well plate by shaking in dark for 20 min. Light absorbance at 550 nm was measured immediately and optical density (OD) values were corrected for an unspecific background on a microplate reader (Tecan Sunrise; Tecan Switzerland).

Proliferation of Schwann cells on TCP, poly-L-lysin (Lysin), EHS laminin-111, pLm-111 or on combinations of poly-L-Lysin with either EHS laminin-111 or pLm-111 was evaluated using a 5-bromo-2-deoxyuridine uptake assay (BrdU; Cell Proliferation ELISA assay Kit; Roche Diagnostics, Switzerland), according to manufacturer's instructions. Briefly, 96-well plates of all groups were seeded with Schwann cells at a density of 4×10^3cells/cm^2 (n = 18). Medium was changed to Schwann cell medium containing 100 µM BrdU and cells were incubated for 24 h at standard cell culture conditions (37 °C and 5% CO_2). The culture plates were fixated with FixDenat® solution and incubated with anti-BrdU POD antibody solution for 45 min at room temperature. After washing the plate with PBS twice, substrate solution containing tetramethyl benzidine was added for 20 min. The reaction was stopped using 1 M H_2SO_4 and absorption was measured at 450 nm with 690 nm as reference wavelength on an automatic microplate reader (Tecan Sunrise; Tecan Switzerland).

1.2.6 NG 108-15 Outgrowth

NG 108–15 cell lines were purchased from ECACC (#88112302, Salisbury, U.K.) and cultured in DMEM high glucose supplemented with 10% FCS, 1% glutamine and 1% Pen/Strep.

24 well plates were incubated with 250 µL of EHS laminin-111 or pLm-111 at 100 µg/mL and UV sterilized for 30 min. Laminin solutions were removed and 12,000 cells were seeded (6000 cells/cm^2, n = 12) on TCP, EHS laminin-111, or pLm-111 in medium supplemented with 20 ng/mL human beta neurotrophic growth factor β -NGF (Peprotech, Vienna, Austria) and incubated at 37 °C. Photographs were taken after 24, 48 and 72 h using an epifluorescence microscope (DMI6000B, Leica GmbH, Vienna, Austria). The neurite outgrowth was analyzed as previously described [33]. Briefly, microscopy pictures were processed in a blinded manner with Adobe

Photoshop software by adjusting contrast/brightness. Then the neurite outgrowth was analyzed using AngioSys software (TCS Cellworks, London, UK). The obtained values were further statistically analyzed using Prism 5 (Graphpad, CA, USA).

1.2.6.1 Immunostaining

For actin/DAPI staining, the medium was aspirated and cells were washed with PBS before fixation in 4% formaldehyde for 10 min. The cells were washed three times with PBS, stained with Alexa Fluor 488 phalloidin (1:40) (Invitrogen) in the dark for 20 min, and washed two additional times with PBS. Then, DAPI staining (1:1000) for 5 min and two additional washing steps were performed before imaging on an epifluorescence microscope (DMI6000B, Leica GmbH, Vienna, Austria).

1.2.7 gfpHUVEC Network Formation

1.2.7.1 Human Umbilical Vein Endothelial Cells (HUVEC) Isolation

HUVEC were isolated from umbilical cords of healthy donors with the authorization of the local ethics committee of Upper Austria with written informed consent of the donors and according to established protocols as previously described [34, 35]. Cells (p6-p9) were cultured in EGM-2 medium (Lonza, Basel, Switzerland) supplemented with 5% FCS. Isolated HUVEC were retrovirally infected with expression vectors for fluorescent proteins using the Phoenix Ampho system as described elsewhere [36].

Network formation was investigated using a previously described vasculogenesis assay [37–39]. Briefly, 50 µL of pLm-111, EHS laminin-111, EHS collagen-4 or calf skin collagen-1 were pipetted per well in 96 well plates at two different concentrations of 500 µg/mL or 1 mg/mL, UV sterilized for 30 min and incubated at 37 °C for 2 h. Coating solutions were removed and 15.000 GFP-HUVECs were seeded (40.000 cells/cm^2, n = 12) in 100 µL of EGM-2 medium. After 48 h of cultivation the networks were imaged and analyzed as previously described [33]. Fluorescence microscopic pictures of two independent experiments (different pLm-111 donors) were taken from two different fields per well and processed in a blinded way using Adobe Photoshop software (Adobe Systems, San Jose, USA) by adjusting contrast/brightness. Then, tube formation was analyzed using AngioSys software (TCS Cellworks, London, UK) and the AngioSys values were analyzed using Prism 5 (Graphpad).

1.3 Data Analysis

All experimental data is presented as mean ± standard deviation (SD) if not stated otherwise. Normal distribution of data was tested with the Kolmogorov–Smirnov test. One-way analysis of variance (ANOVA) with Tukey's post hoc test was used to calculate statistical significance. For the NG108-15 outgrowth assay, a Two-Way ANOVA with Bonferroni post-test was used. P-values <0.05 were considered statistically significant. All calculations were performed using GraphPad software (GraphPad software, Inc., San Diego, CA, USA).

1.4 Results

1.4.1 Extraction of pLm-111 from Placenta

1.4.1.1 Yield and Purity

We have developed an effective method for isolating pLm-111 by extraction with a Tris-NaCl buffer combined with non-protein-denaturizing ammonium sulfate precipitation and rapid tangential flow filtration steps.

A detailed flow chart of the method is shown in Fig. 1.1. After defrosting, the chorionic membrane was removed and basal villous tissue was isolated. Major blood components were removed using PBS buffer/aqua dest. Thereafter, collagen remnants were removed and the residual laminin-111 diafiltrated against physiologic TBS buffer. The mean amount of *pLm-111* after isolation was

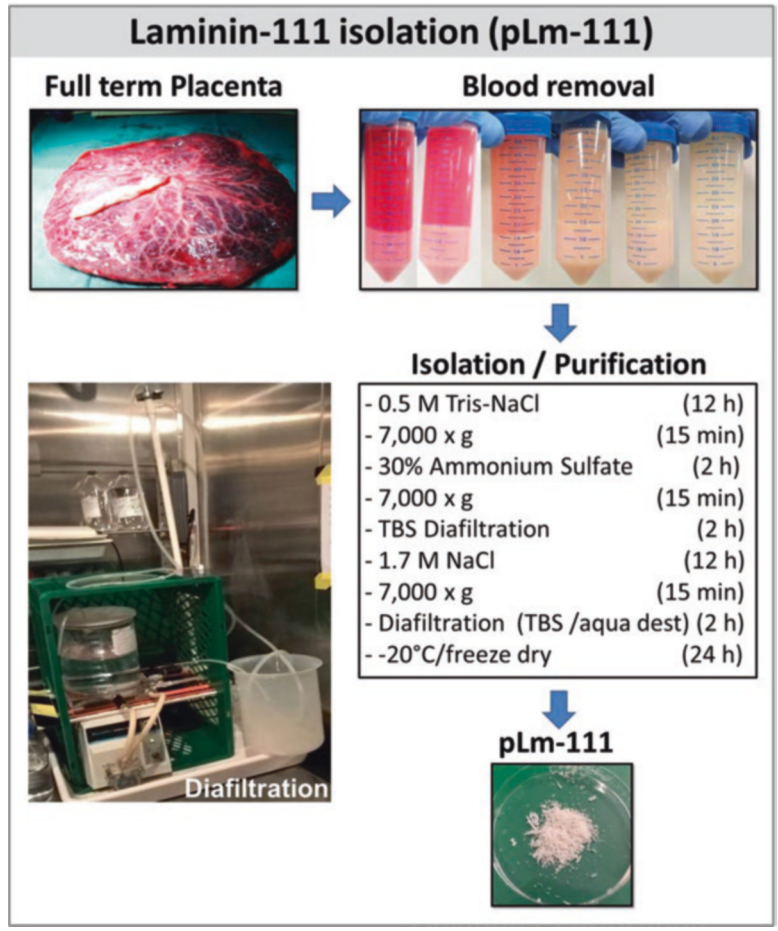

Fig. 1.1 Graphical overview of steps required for the introduced rapid and efficient isolation of laminin-111 from human placenta (pLm-111). *Full term placenta* is dissected free of amnion/chorion followed by centrifugation to *remove blood components*, and further *isolation/purification* steps (salt-precipitation and diafiltration) to separate laminin-111. Final freeze-drying leads to powdery laminin-111 isolates

175 ± 35 mg/100 g wet weight basal tissue (n = 7).

By the use of Dot blot and monoclonal antibodies we assessed the presence of native laminin-111 in TBS buffer (Fig. 1.2a). After diafiltration and freeze-drying, laminin-111 is denatured and is therefore not detectable by the used monoclonal antibody (Fig. 1.2b). By using SDS-PAGE gels stained with Coomassie blue we assessed major protein bands in lyophilized pLm-111 (Fig. 1.2c) between 200 and 300 kDa. In western blot analysis using polyclonal antibodies, laminin-111 bands were clearly detected and matching with the major bands from the SDS-PAGE (Fig. 1.2d).

Table 1.1 lists the amino acid composition of human laminin-111 α, β and γ-chains (www.uniprot.org), pLm-111 from three different donors and the amino-acid composition of EHS collagen-4 and human collagen-4 from placenta.

1.4.2 Biocompatibility of pLm-111

1.4.2.1 Schwann Cell Viability

The MTT assay was used to analyze Schwann cell viability on pLm-111 compared to EHS laminin-111. Cell viability on all three single coatings was significantly increased compared to the TCP control group (OD values: lysin 1536 ± 220, EHS laminin-111 1776 ± 195, pLm-111 1763 ± 216, TCP 503 ± 42, n = 18, Fig. 1.3a) but no significant difference among the three coating groups could be detected (p = 0.78). Schwann cells cultured on both combined coatings of lysin and EHS laminin-111 or lysine and pLm-111

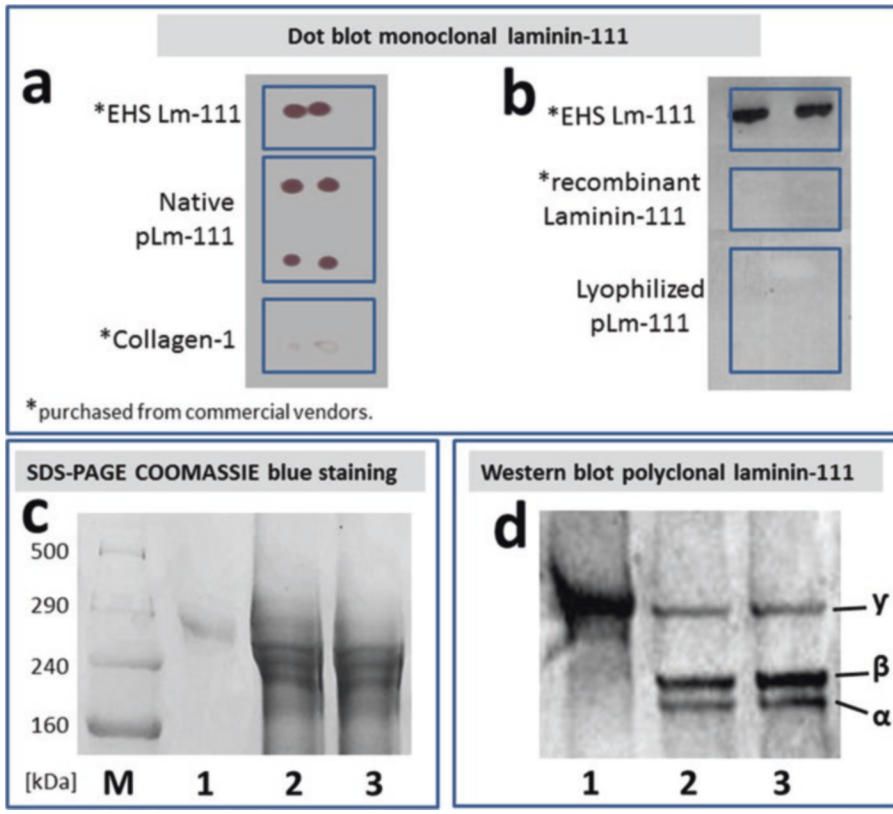

Fig. 1.2 Isolated laminin-111 characterized by (**a**) Representative immunoblot of duplicates of 2 μg of purchased Engelbreth-Holmes Sarcoma (EHS) laminin-111, isolated native pLm-111 from two independent donors, purchased collagen-1 from rat tail against a monoclonal laminin-111 antibody. (**b**) Representative immunoblot showing duplicates of 2 μg of cell culture laminin-111, EHS laminin-111 or lyophilized pLm-111 from two independent donors against a polyclonal laminin-111 antibody. (**c**) Coomassie blue stained 3–8% SDS-polyacrylamide gel showing marker (M) (HiMark, Life Technologies), (1) EHS laminin-111 and (2, 3) two independent lyophilized pLm-111 isolates from two different donors. (**d**) Corresponding immunoblot showing 20 μg of (1) EHS laminin-111 and (2, 3) two independent lyophilized pLm-111 isolates from two independent donors loaded per lane and a primary antibody against polyclonal laminin-111

showed increased viability (between 33% and 46%) compared to the single coatings or the TCP control. There were no significant differences between lysin/EHS laminin-111 and lysin/pLm-111 (OD values: lysin/EHS laminin-111 2285 ± 230, lysin/pLm-111 2362 ± 216, p = 0.75).

The results of the proliferation analysis were similar to the viability assays. Schwann cells show higher proliferation on all three single coatings, compared to TCP (OD values: Lysin 3681 ± 512, EHS Laminin-111 3722 ± 470, pLm-1,113,822 ± 474, TCP 1871 ± 122, n = 18, Fig. 1.3b). No significant difference could be observed between the single coating groups (p = 0.87). Proliferation on combined coating of lysine and EHS laminin-111 or lysine and pLm-111 resulted in increased proliferation (between 23% and 33%) compared to the single coatings or the TCP but no differences between EHS laminin-111 and pLm-111 were detectable (OD values: EHS Laminin-111 4938 ± 297, pLm-111 5034 ± 381, p = 0.79).

1.4.2.2 NG 108-15 Outgrowth

An outgrowth assay was used to analyze NG 108–15 cells on pLm-111 compared with EHS laminin-111 (Fig. 1.4). After 24 h, the total neurite outgrowth (TCP 86 ± 3 μm, EHS

Table 1.1 Amino acid composition of pLm-111 (mean ± SD) from human placenta (Residues per 1.000 total amino acids residues)

	Human laminin-111[a]					
Amino acids	α laminin-111	β laminin-111	γ laminin-111	pLm-111 (mean ± SD, n = 3)	EHS tumor collagen-4 [57]	Human collagen-4 [58]
Alanine	61.4	66.6	86.4	73.1 ± 1.4	45	33.5
Arginine	50.1	49.3	59.7	48.1 ± 2.8	30	30.5
Aspartic acid	102.7	110.9	128	76.1 ± 5	52	53.5
Cystine	52.3	71.1	62.2	51.6 ± 5.2	7	–
Glutamic acid	131.7	136.1	129.9	94.1 ± 5.1	103	100.5
Glycine	80.3	70.5	70.2	105.4 ± 10.9	280	339
Histidine	28.7	21.8	16.8	16.0 ± 0.8	11	7.6
Hydroxyproline	–	–	–	16.1 ± 2.4	102	97
Isoleucine	38.7	39.2	30.5	39.6 ± 1.6	25	30.5
Leucine	91	76.7	73.3	72.5 ± 3.5	54	52.5
Lysine	44.7	47.6	50.3	46.2 ± 4.6	49	58.6
Methionine	12.6	17.9	13.7	51.1 ± 8.7	12	12
Phenylalanine	27.1	30.8	30.5	28.5 ± 1.3	31	30
Proline	46	48.7	44.1	57.8 ± 0.7	66	87.5
Serine	76.9	67.2	61.5	59.6 ± 2.4	60	12.5
Threonine	53.9	52.1	60.3	49.1 ± 2.1	34	17
Tryptophane	7.6	7.3	6.8	4.4 ± 1.3	–	–
Tyrosine	30.9	31.4	28	26 ± 1.6	9	9.8
Valine	63.6	54.9	47.9	84.6 ± 2.9	30	28
Total	1.000	1.000	1.000	1.000	1.000	1.000

Table contains amino acid analysis of pLM-111 isolates (n = 3) and reference values for human laminin-111, EHS tumor collagen 4 and human collagen 4 as control
[a]amino acid quantification according to www.uniprot.org

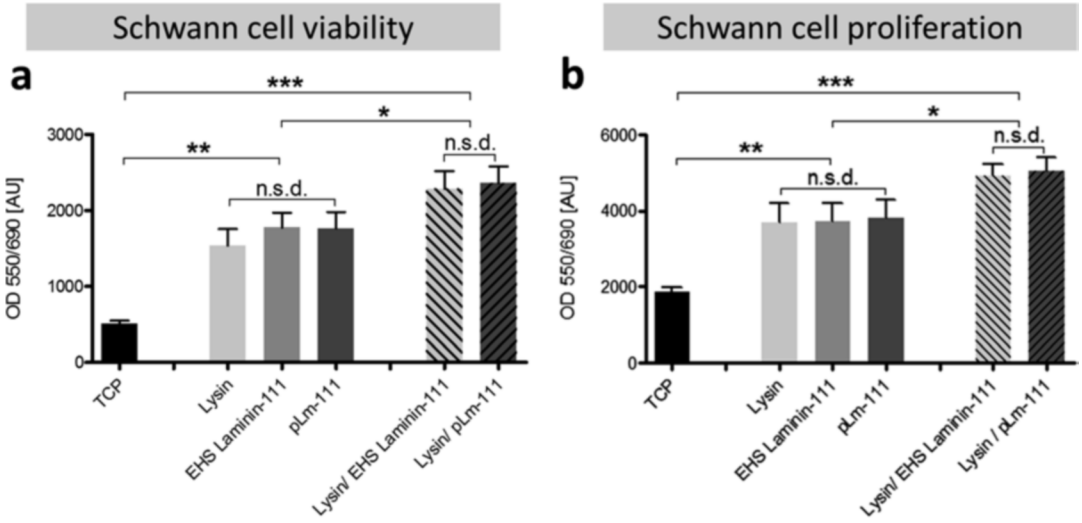

Fig. 1.3 Schwann cell viability (MTT assay) and proliferation (BrdU assay) 24 h after seeding on tissue culture plastic (TCP) compared to EHS laminin-111 and pLm-111 coated wells (100 µg/mL), as well as poly-L-lysin/EHS laminin-111 and poly-L-lysin/pLm-111. Data is presented as mean + SD; significance tested with 1-way ANOVA followed by Tukey's post test; *,** and *** indicates significant difference of $p < 0.05$, 0.01 and 0.005, respectively; n = 18

laminin-111,268 ± 13 µm, pLm-111,519 ± 16 µm, n = 12) and the number of tubules (TCP 5 ± 1, EHS laminin-111 11 ± 3, pLm-111 20 ± 2, n = 12) on pLm-111 were significantly increased compared to the TCP control and EHS laminin-111, but no significant difference between EHS laminin-111 and TCP could be detected. After 48 h, the total neurite outgrowth (TCP 71 ± 6 µm, EHS laminin-111,590 ± 110 µm, pLm-111,848 ± 240 µm, n = 12) and the number of tubules (TCP 3 ± 1, EHS laminin-111 21 ± 5, pLm-111 33 ± 9, n = 12) on both coatings were significantly increased compared to the TCP control, but no significant difference between EHS laminin-111 and pLm-111 could be detected. After 72 h, the total neurite outgrowth (TCP 96.9 ± 1 µm, EHS laminin-111,382 ± 4 µm, pLm-111 1024 ± 6 µm, n = 12) and the number of tubules (TCP 6 ± 1, EHS laminin-111 20 ± 4, pLm-111 47 ± 5, n = 12) on pLm-111 were significantly increased compared to EHS laminin-111.

1.4.2.3 HUVEC Network Formation

A well-established vasculogenesis assay was used to analyze gfpHUVEC with fully supplemented EGM-2 medium on pLm-111 from two independent isolations (donors D1; D2) and compared with EHS laminin-111 (Fig. 1.5). After 24 h, a cell network was formed on EHS laminin-111 and pLm-111 at 1 mg/mL but neither on EHS collagen-4 nore on lower pLm-111 coating concentrations or TCP. After 48 h, the networks were analyzed. There was no significant difference between the number of tubules (EHS laminin-111,134 ± 17, pLm-111 D1 124 ± 13; D2 157 ± 18, n = 12) or the total tubule length (EHS laminin-111 35 ± 6 mM, pLm-111 D1 37 ± 2; D2 42 ± 5 mM, $p < 0.5$, n = 12) between both laminin-111 coatings. The mean tubule length (EHS laminin-111,240 ± 7 µm, pLm-111 D1 315 ± 17; D2 300 ± 13 µm, n = 12) and the number of junctions (EHS laminin-111,284 ± 28, pLm-111 D1 410 ± 42; D2 463 ± 47, n = 12) were significantly increased on pLm-111 compared to EHS laminin-111.

1.5 Discussion

Although laminin-111 from EHS tissue was already described more than 30 years ago, about 20,000 laminin publications in 2016 proved the ongoing interest in this key protein [2].

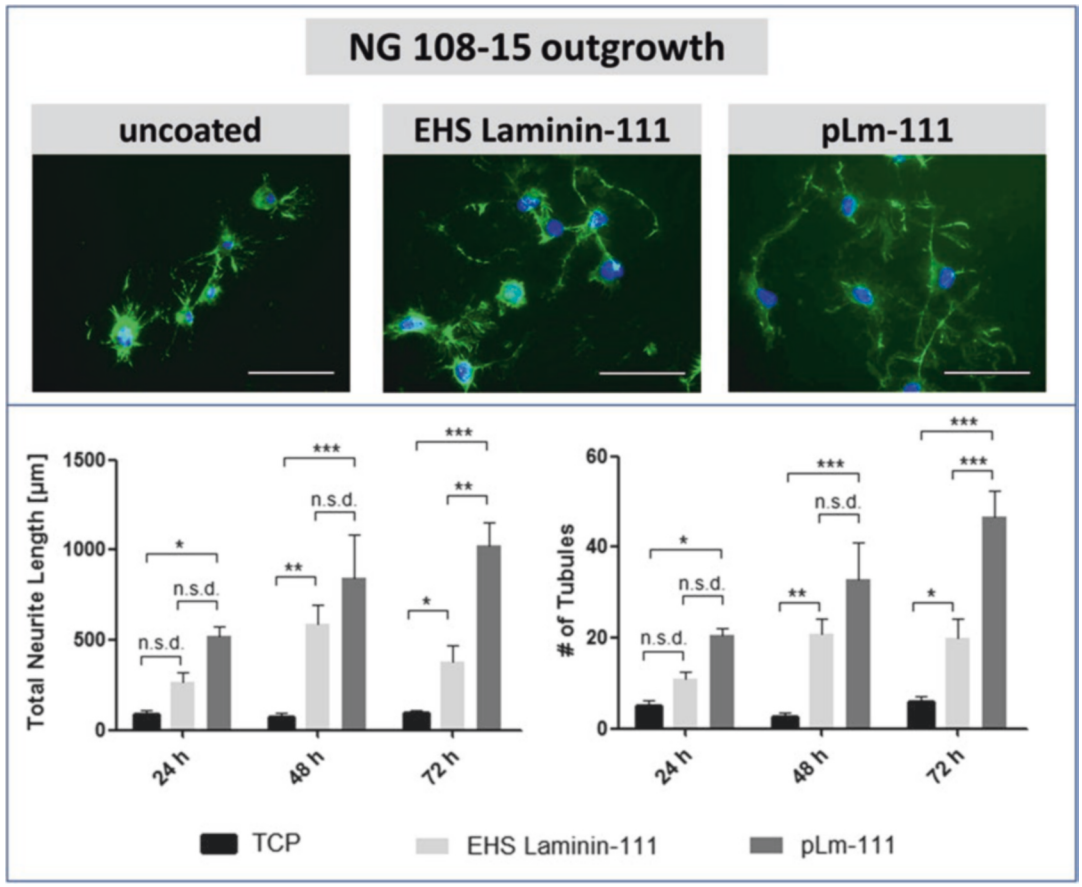

Fig. 1.4 Upper panel: fluorescence micrographs of phalloidin (green) and DAPI (blue) stained NG 108-15 cells cultivated on tissue culture plastic (TCP), EHS laminin-111 or pLm-111 at concentrations of 100 µg/mL; Scale bars = 100 µm; Lower panel: analysis of the neurite outgrowth: total neural length and number of tubules per field of view of NG108 cells after 24, 48 and 72 h of cultivation. Data is presented as mean + SD; significance tested with 2-way ANOVA followed by Bonferroni post test; *,** and *** indicate significant difference of $p < 0.05$, 0.01 and 0.005, respectively; n = 12

Laminin-111 is naturally present during embryonic development and has been shown to be a useful biomaterial for the cultivation of stem cells [7, 26, 40, 41]. Beside, it has been used for various applications in tissue engineering and regenerative medicine, eg. cultivation of neuronal cells [7, 11], angiogenesis studies [5, 13], or wound healing studies [6, 15]. A robust method for culturing human pluripotent stem cells under xeno-free conditions is an important tool for stem cell research and for the development of regenerative medicine [42]. Especially in the research of muscle tissue biology, laminin-111 has been shown to improve skeletal muscle stem cell quality and function [43]. In this regard, *Goudenne et al.* could demonstrate that intramuscular injection of laminin-111 increased muscle strength and resistance in mice and could potentially be used to treat Duchenne muscular dystrophy [44].

Regarding clinical applicability, caution must be taken regarding the tissue origin of the extracted biomaterials. Proteins extracted from xenogenic tumor tissues are not suitable for clinical applications. Non-human proteins are reported to provoke immune responses in patients [45], and carry the risk of xenogenic disease transmission [46, 47]. Therefore, human sources are regarded as the best option for the generation of medicinal products [30]. In this regard, human placenta is a highly vascularized organ [48], and

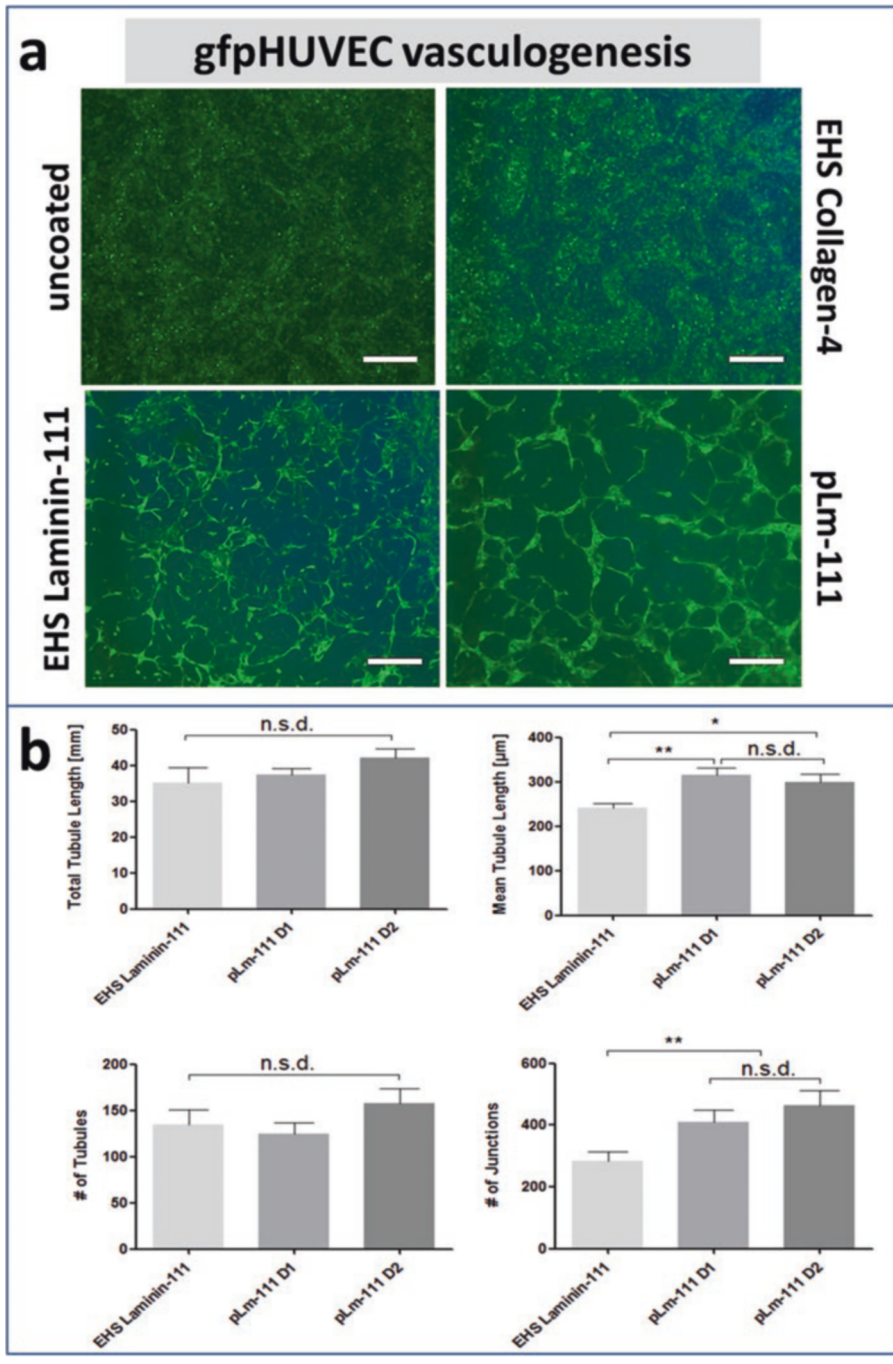

Fig. 1.5 pLm-111 at higher concentrations promotes vasculogenesis using gfpHUVEC (**a**) Fluorescence micrographs of gfpHUVEC 48 h after seeding on EHS laminin-111, pLm-111, or EHS collagen-4 at concentrations of 1 mg/mL. Scale bar = 400 µm. (**b**) Network characteristics (total/mean tube length, number of junctions/tubules) of gfpHUVEC, seeded on EHS laminin-111 or pLm-111 from two independent donors (pLm-111 D1; D2). Data is presented as mean + SD; significance tested with 1-way ANOVA followed by Tukey's post test; *,** and *** indicates significant difference of $p < 0.05$, 0.01 and 0.005, respectively; n = 12

it therefore harbors high amounts of basal membrane proteins [49]. Human placenta tissue is available in sufficient amounts and consistent quality for large industrial scale processes. Moreover, it has been shown to exhibit excellent anti-inflammatory and antibacterial properties, [50] which has been favoring its use to treat non-healing wounds for decades [51–53].

Commercial success of a medicinal product is dependent on the balance of efficacy and cost-effectivness [54]. Several studies have been performed to isolate laminin isoforms from placenta using salt precipitation or pepsin digestion and chromatography [20–24]. However, the protocols to isolate laminin-111 described in the literature to date are time consuming, work intensive and show low extraction efficiency. By modifying the protocols described in literature, we were able to (1) significantly increase the extraction efficiency of laminin-111 yield from placenta tissue compared to reported isolation protocols and (2) to shorten the isolation time from almost 2 weeks to a total of only 4 processing days (Fig. 1.1) [20–22]. In our protocols, tangential flow filtration instead of dialysis was used since it was less time-consuming and further allows easy and rapid concentration of laminin isolates. Collagen-4 remnants were removed by precipitation with 1.7 M NaCl [18].

Native laminin-111 from human placenta was assessed using Dot Blots. Residual salts from TBS buffer were removed by tangential flow filtration against aqua dest and the proteins were freeze-dried to make process ability and storage easier. On the average, 175 ± 35 mg of laminin-111 was isolated from 100 g of placenta tissue using the isolation protocol described here. In western blot analysis for laminin-111 and SDS-PAGE analysis, two bands around 200 kDa were clearly visible, which represent the α1 and ß1 chains, as described in literature [1, 19, 55]. Interestingly, a third protein band was visible with a molecular weight of approximately 300 kDa in both the pLm-111 isolates and in EHS laminin used as control. This high molecular weight band most likely represents the reduced γ-chain, which usually appears around 400 kDa [2, 19]. The HPLC- based amino acid quantification analysis is consistent with the data from www.uniprot.com, however low amounts of hydroxyproline were still detectable. Most probably, these could be attributed to impurities of the isolate with collagen-4, another major component of BMs beside laminin [55].

Freeze-dried pLm-111 was used as a coating substrate and compared to xenogenic standard proteins using Schwann cells. These experiments indicated that the pLm-111 isolates show bioactivity comparable to commercially available xenogenic proteins. Furthermore, pLm-111 promoted rapid attachment of various cells including Schwann cells, HUVEC or NIH3T3 fibroblasts (data not shown). NG 108-15 cells rapidly developed a complex neurite outgrowth on pLm-111 with at least similar effectiveness compared to xenogenic proteins.

In addition, laminin-111 is the principal factor for endothelial cells to differentiate into interconnected tubules on Matrigel, a laminin-111-rich (around 70%) gel, extracted from basement membrane tumor materials from mice [56]. However, beside its tumorigenic origin, Matrigel is a heterogenic mixture of various extracellular matrix proteins and pro-angiogenic growth factors. For potential clinical applications, a single protein would be an advantageous material. EHS laminin-111 at concentrations of 1 mg/mL promotes the differentiation of gfpHUVEC into interconnected networks, but so does pLm-111 from human origin with at least similar performance (total/mean tube length, number of tubules/junctions).

The 2D cell culture experiments described above have been performed with freeze-dried laminin-111 stored at −20 °C for at least 6 months. Moreover, in other *in vitro* experiments we have used the isolated lyophilized pLm-111 materials after storing them for up to 18 months without noticing alterations in stability or activity (data not shown).

To conclude, we could establish a simple, rapid and effective method to isolate laminin-111 from human placenta. This pLm-111 clearly demonstrates its applicability as a biomaterial of human origin with strong bioactive potential for a broad spectrum of *in vitro* and potentially *in vivo* tissue engineering approaches.

1.6 Conclusion

Summarizing, we established an effective method for isolating laminin-111 from human placenta, a clinical waste material. Laminins are routinely used in cell culture to on the one hand improve attachment of cells (eg Schwann cells), and on the other hand induce specific functions (eg HUVEC). The availability of this potent and versatile protein offers new, fully human, approaches for neuronal and endothelial *in vitro* tissue engineering and may provide a new platform technology for clinical use with an increased overall safety profile for patients.

Acknowledgement The authors acknowledge Red Cross Blood Transfusion Service, Linz, Upper Austria for providing the placenta tissue, Dr. Wolfgang Holnthoner, Severin Mühleder, MSc, for providing the HUVEC and Mag. med. vet. James Ferguson for reviewing the manuscript. This work was partially funded by the City of Vienna Competence Team Tissue Engineering Signaltissue (MA23 Project-#18-08).

Disclosure Statement None.

References

1. Aumailley M (2013) The laminin family. Cell Adhes Migr 7:48–55
2. Simon-Assmann (2013) The laminin family. Cell Adhes Migr 7:44–47
3. Ekblom P, Lonai P, Talts JF (2003) Expression and biological role of laminin-1. Matrix Biol 22:35–47
4. Hozumi K et al (2012) Reconstitution of laminin-111 biological activity using multiple peptide coupled to chitosan scaffolds. Biomaterials 33:4241–4250
5. Ponce ML, Kleinman HK (2003) Identification of redundant angiogenic sites in laminin α1 and γ1 chains. Exp Cell Res 285:189–195
6. Iorio V, Troughton LD, Hamill KJ (2015) Laminins: roles and utility in wound repair. Adv Wound Care 4:250–263
7. Flanagan L a, Rebaza LM, Derzic S, Schwartz PH, Monuki ES (2006) Regulation of human neural precursor cells by laminin and integrins. J Neurosci Res 83:845–856
8. Madison R, da Silva CF, Dikkes P, Chiu TH, Sidman RL (1985) Increased rate of peripheral nerve regeneration using bioresorbable nerve guides and a laminin-containing gel. Exp Neurol 88:767–772
9. Bilozur ME, Hay ED (1988) Neural crest migration in 3D extracellular matrix utilizes laminin, fibronectin, or collagen. Dev Biol 125:19–33
10. Rangappa N, Romero A, Nelson KD, Eberhart RC, Smith GM (2000) Laminin-coated poly(L-lactide) filaments induce robust neurite growth while providing directional orientation. J Biomed Mater Res 51:625–634
11. Biernaskie J et al (2007) Skin-derived precursors generate myelinating Schwann cells that promote remyelination and functional recovery after contusion spinal cord injury. J Neurosci 27:9545–9559
12. Kidd KR, Williams SK (2004) Laminin-5-enriched extracellular matrix accelerates angiogenesis and neovascularization in association with ePTFE. J Biomed Mater Res A 69:294–304
13. Malinda KM, Wysocki AB, Koblinski JE, Kleinman HK, Ponce ML (2008) Angiogenic laminin-derived peptides stimulate wound healing. Int J Biochem Cell Biol 40:2771–2780
14. Min SK et al (2010) The effect of a laminin-5-derived peptide coated onto chitin microfibers on re-epithelialization in early-stage wound healing. Biomaterials 31:4725–4730
15. Hashimoto T, Suzuki Y, Tanihara M, Kakimaru Y, Suzuki K (2004) Development of alginate wound dressings linked with hybrid peptides derived from laminin and elastin. Biomaterials 25:1407–1414
16. Gjorevski N et al (2016) Designer matrices for intestinal stem cell and organoid culture. Nat Publ Gr 539:560–564
17. Horejs C-M et al (2014) Biologically-active laminin-111 fragment that modulates the epithelial-to-mesenchymal transition in embryonic stem cells. Proc Natl Acad Sci USA 111:5908–5913
18. Timpl R, Rohde H, Robey PG, Rennard SI, Foidart JM, Martin GR (1979) Laminin-A glycoprotein from basement membranes. Biochemistry 21:6188–6193
19. Aumailley M, Smyth N (1998) The role of laminins in basement membrane function. J Anat 193(Pt 1):1–21
20. Brown JC, Spragg JH, Wheeler GN, Taylor PW (1990) Identification of the B1 and B2 subunits of human placental laminin and rat parietal-yolk-sac laminin using antisera specific for murine laminin-beta-galactosidase fusion proteins. Biochem J 270:463–468
21. Brown JC, Wiedemann H, Timpl R (1994) Protein binding and cell adhesion properties of two laminin isoforms (AmB1eB2e, AmB1sB2e) from human placenta. J Cell Sci 107(Pt 1):329–338
22. Wewer U et al (1983) Human laminin isolated in a nearly intact, biologically active form from placenta by limited proteolysis. J Biol Chem 258(20):12654–12660
23. Engvall E, Earwicker D, Haaparanta T, Ruoslahti E, Sanes JR (1990) Distribution and isolation of four laminin variants; tissue restricted distribution of heterotrimers assembled from five different subunits. Cell Regul 1:731–740
24. Champliaud MF et al (2000) Posttranslational modifications and beta/gamma chain associations of human laminin alpha1 and laminin alpha5 chains: purification of laminin-3 from placenta. Exp Cell Res 259:326–335

25. Cameron K et al (2015) Recombinant laminins drive the differentiation and self-organization of hESC-derived hepatocytes. Stem Cell Rep 5:1250–1262
26. Miyazaki T et al (2008) Recombinant human laminin isoforms can support the undifferentiated growth of human embryonic stem cells. Biochem Biophys Res Commun 375:27–32
27. Wondimu Z et al (2006) Characterization of commercial laminin preparations from human placenta in comparison to recombinant laminins 2 (α2β1γ1), 8 (α4β1γ1), 10 (α5β1γ1). Matrix Biol 25:89–93
28. Weihs AM et al (2014) Shock wave treatment enhances cell proliferation and improves wound healing by ATP release-coupled extracellular signal-regulated kinase (ERK) activation. J Biol Chem 289:27090–27104
29. Duhamel RC (1983) Differential staining of collagens and non-collagens with Coomassie brilliant blue G and R. Coll Relat Res 3:195–204
30. Hackethal J et al (2017) An effective method of *Atelocollagen* type 1/3 isolation from human placenta and its *in vitro* characterization in two-dimensional and three-dimensional cell culture applications. Tissue Eng Part C Methods 23:274–285
31. Schuh CMAP et al (2016) Extracorporeal shockwave treatment: a novel tool to improve Schwann cell isolation and culture. Cytotherapy 18:760–770
32. Kaewkhaw R, Scutt AM, Haycock JW (2012) Integrated culture and purification of rat Schwann cells from freshly isolated adult tissue. Nat Protoc 7:1996–2004
33. Holnthoner W et al (2012) Adipose-derived stem cells induce vascular tube formation of outgrowth endothelial cells in a fibrin matrix. J Tissue Eng Regen Med 4:524–531
34. Rohringer S et al (2017) The impact of wavelengths of LED light-therapy on endothelial cells. Sci Rep 7:1–11
35. Holnthoner W et al (2017) Endothelial cell-derived extracellular vesicles size-dependently exert procoagulant activity detected by thromboelastometry. Sci Rep 7:1–9
36. Knezevic L et al (2017) Engineering blood and lymphatic microvascular networks in fibrin matrices. Front Bioeng Biotechnol 5:1–12
37. Arnaoutova I, Kleinman HK (2010) In vitro angiogenesis: endothelial cell tube formation on gelled basement membrane extract. Nat Protoc 5:628–635
38. Uriel S et al (2009) Extraction and assembly of tissue-derived gels for cell culture and tissue engineering. Tissue Eng Part C Methods 15:309–321
39. Goodwin AM (2007) In vitro assays of angiogenesis for assessment of angiogenic and anti-angiogenic agents. Microvasc Res 74:172–183
40. Sorkio A et al (2014) Structure and barrier properties of human embryonic stem cell-derived retinal pigment epithelial cells are affected by extracellular matrix protein coating. Tissue Eng Part A 20:622–634
41. Takayama K et al (2013) Long-term self-renewal of human ES/iPS-derived hepatoblast-like cells on human laminin 111-coated dishes. Stem Cell Rep 1:332–335
42. Rodin S, Antonsson L, Hovatta O, Tryggvason K (2014) Monolayer culturing and cloning of human pluripotent stem cells on laminin-521–based matrices under xeno-free and chemically defined conditions. Nat Protoc 9:2354–2368
43. Zou K, DeLisio M (2014) Laminin-111 improves skeletal muscle stem cell quantity and function following eccentric exercise. Stem Cells Transl Med 3:1013–1022
44. Goudenege S et al (2010) Laminin-111: a potential therapeutic agent for Duchenne muscular dystrophy. Mol Ther 18:2155–2163
45. Flynn L, Hrabchak C, Woodhouse KA (2006) Biological skin substitutes for wound cover and closure. Expert Rev Med Devices 3(3):1–20
46. Pacak C a, MacKay A, Cowan DB (2014) An improved method for the preparation of Type I collagen from skin. J Vis Exp 83:e51011
47. Browne S, Zeugolis DI, Pandit A (2013) Collagen: finding a solution for the source. Tissue Eng Part A 19:1491–1494
48. Schneider KH et al (2016) Decellularized human placenta chorion matrix as a favorable source of small-diameter vascular grafts. Acta Biomater 29:125–134
49. Wang Y, Zhao S (2010) Vascular biology of the placenta, vol 2. Morgan & Claypool LIFE Sciences, San Rafael, p 1
50. Lobo SE et al (2016) The placenta as an organ and a source of stem cells and extracellular matrix: a review. Cells Tiss Org 270:239–252
51. Burgos H, Herd A, Bennett JP (1989) Placental angiogenic and growth factors in the treatment of chronic varicose ulcers: preliminary communication. J R Soc Med 82:598–599
52. Shukla VK, Rasheed M a, Kumar M, Gupta SK, Pandey SS (2004) A trial to determine the role of placental extract in the treatment of chronic non-healing wounds. J Wound Care 13:177–179
53. Navadiya SK, Vaghani YL, Patel MP (2012) Study of topical placental extract versus povodine iodine and saline dressing in various diabetic wounds. Nat J Med Res 2:411–413
54. Place ES, Evans ND, Stevens MM (2009) Complexity in biomaterials for tissue engineering. Nat Mater 8:457–470
55. Kleinman HK et al (1982) Isolation and characterization of type IV procollagen, laminin, and heparan sulfate proteoglycan from the EHS sarcoma. Biochemistry 21:6188–6193
56. Kubota Y, Kleinman HK, Martin GR, Lawley TJ (1988) Role of laminin and basement membrane in the morphological differentiation of human endothelial cells into capillary-like structures. J Cell Biol 107:1589–1598
57. Timpl R, Martin GR, Bruckner P, Wick G, Wiedemann H (1978) Nature of the collagenous protein in a tumor basement membrane. Eur J Biochem 84:43–52
58. MacWright RS, Benson V a, Lovello KT, van der Rest M, Fietzek PP (1983) Isolation and characterization of pepsin-solubilized human basement membrane (type IV) collagen peptides. Biochemistry 22:4940–4948

2 A Novel Strategy for Simple and Robust Expansion of Human Pluripotent Stem Cells Using Botulinum Hemagglutinin

Mee-Hae Kim and Masahiro Kino-oka

Abstract

Clinical and industrial application of human pluripotent stem cells (hPSCs) has been hindered by the lack of robust strategies to sustain cultures in an undifferentiated state. Here, we describe a simple and robust method to culture and propagate hPSCs, which we anticipate will remove major roadblocks in investigating the basic properties of undifferentiated hPSCs and accelerate cell-based manufacturing. We also provide an overview of the use of botulinum hemagglutinin, an inhibitor of E-cadherin, to maintain and expand various hPSC lines in an undifferentiated state in different culture conditions. Hemagglutinin selectively removes cells that have lost the undifferentiated state, dissociates aggregates *in situ*, and is easy to use, scalable, and reproducible.

Keywords

Human pluripotent stem cells · Botulinum hemagglutinin · E-cadherin disruption · Removal of differentiated cells · Undifferentiated state · High-density culture · Suspension culture

M.-H. Kim · M. Kino-oka (✉)
Department of Biotechnology, Graduate School of Engineering, Osaka University, Suita, Osaka, Japan
e-mail: mh-kim@bio.eng.osaka-u.ac.jp; kino-oka@bio.eng.osaka-u.ac.jp

2.1 Introduction

Human pluripotent stem cells (hPSCs), including human embryonic stem cells (hESCs) and human induced pluripotent stem cells (hiPSCs), hold great clinical and industrial potential, because of unlimited self-renewal in culture and capacity to differentiate into any cell type [18, 44, 45]. Although methods to optimize hPSC expansion and differentiation have advanced considerably, efficiency, reproducibility, and product quality are ongoing challenges [14].

In two-dimensional monolayer culture, hiPSCs spontaneously lose the undifferentiated state, *i.e.*, deviate from the undifferentiated state, dramatically transforming into large, flat cells [15–17] that gradually take over the colony with passage, and eventually the entire culture vessel. The nature of these cells remains unclear; for example, it is not known whether expression of lineage markers in these cells is only sporadic or a coherent departure from pluripotency. Although spontaneous loss of the undifferentiated state is expected and signifies pluripotency, it may interfere with culture maintenance and intended use if left uncontrolled. Thus, several strategies have been proposed to eliminate these cells based on morphological features [35, 48]. However, as morphological analysis is subjective, industrial-scale cell production would probably require methods independent of individual experts.

In conventional three-dimensional suspension culture, hiPSCs form aggregates that grow in size

H. J. Chun et al. (eds.), *Novel Biomaterials for Regenerative Medicine*, Advances in Experimental Medicine and Biology 1077, https://doi.org/10.1007/978-981-13-0947-2_2

over time [1, 4, 27, 34]. However, these aggregates also deposit a collagen-rich shell that, along with mass transport limitations, impedes the delivery of oxygen and essential nutrients, especially in larger aggregates of highly metabolically active cells, and results in necrosis and differentiation [46, 50]. To address this issue, alternative methods were recently described [1, 2, 4], and stirred culture systems such as spinner flasks and stirred-tank bioreactors are also widely used [2, 11, 29, 32, 33, 52]. In addition, several factors such as inoculation density, medium composition, and culture conditions can be manipulated as needed. Nevertheless, lack of understanding of the nature of hPSC aggregates in suspension culture, and of a scalable method for long-term propagation, limits usefulness.

Considering the biological differences between undifferentiated cells and deviated cells in monolayers, as well as physiological changes during aggregate growth in suspension, we hypothesized that disruption of the epithelial barrier may facilitate the maintenance and expansion of undifferentiated cells. To this end, *Clostridium botulinum* hemagglutinin, a component of the large botulinum neurotoxin complex that directly binds E-cadherin and disrupts cell–cell adhesion at adherens junctions [23, 40–42], may be useful.

In this chapter, we first introduce fundamental mechanisms related to the maintenance and expansion of undifferentiated hiPSCs, as inferred from morphological and biological features. We then review recent advances in hPSC culture strategies, as well as in experimental approaches to investigate hPSC physiology, with an emphasis on the application and the industrial and clinical potential of hemagglutinin-based processing of cells and tissues.

2.2 Principles Underlying the Maintenance and Expansion of Undifferentiated hPSCs

Based on a growing body of research, cell-cell and cell-substrate interactions are now known to influence commitment and differentiation in hPSCs. Indeed, hESC and hiPSC colonies exhibit structural characteristics of polarized epithelial cells, and form cell-cell adhesions via E-cadherin and integrin [22, 38]. This dynamic structure physically connects neighboring cells, couples intercellular adhesive contacts to the cytoskeleton, and helps define the apical-basal axis in each cell [3, 6, 26]. Cell-cell and cell-substrate adhesions are also spatially regulated and coordinated [20], such as by interactions between actin and Rho GTPases, membrane turnover and trafficking, and interplay between cell-cell and cell-substrate adhesion [9, 21]. In addition, the Ras GTPase Rap1 regulates endocytic membrane recycling to control cell junctions and stabilize apical-basal polarity, both of which are essential for colony formation and self-renewal [19, 24, 25, 36]. Indeed, Rap1 coordinates E-cadherin, integrin, and cytoskeleton reorganization, and restores hiPSC structure and function after loss of E-cadherin. Collectively, these studies provide not only critical insights into the behavior of undifferentiated hiPSCs, but also unique and powerful opportunities to culture and maintain stem cells.

2.2.1 Mechanism of Loss of Undifferentiated State in Monolayer Culture

Proposed mechanisms for the spontaneous and dramatic loss of the undifferentiated state in monolayer culture are illustrated in Fig. 2.1 [12,13,16] for hiPSC colonies cultured on SNL and MEF feeder cells. On SNL feeder cells, hiPSCs grow outward, with cells simultaneously dividing and migrating, gradually becoming larger and more tightly packed (Fig. 2.1a). Consequently, cell motility steadily decreases while the cell density at the center increases. Notably, central cells then partially detach from the substrate, exhibit morphological changes consistent with apoptosis, enlarge, and flatten. It appears that the contraction of a blebbing apoptotic cell drags neighboring cells into the space it vacates, thereby inducing loss of undifferentiated state. Ultimately, a large number of cells dissociate from colonies and disperse as single cells.